Monte Carlo Study of Multicritical Behavior of the 3D Anisotropic Heisenberg Model

by

Siyan Hu

(Under the direction of David Landau)

Abstract

The uniaxially anisotropic $3D$ Heisenberg antiferromagnet model in an external field has been attracted great interest during recent decades, in particular, in its structures and phase transition behaviors in an applied magnetic field. It has been known that it displays an antiferromagnet (AF) phase (where spins from two sublattices tend to be aligned in opposite directions along the z axis) in low field and temperature and a spin-flop (SF) phase (where spins from two sublattices have the same z components but opposite xy components) and paramagnetic (P) phase (where spins are aligned in the same z direction). The meeting point of three phases is the multicritical point, however, the nature of the multicritical point has been controversial. It has been suspected that there exists a biconical structure between the AF and SP phase, and, the bicritical point is substituted with a tetracritical point. We study the phase transition near the multicritical point using Monte Carlo simulation to detect any evidence of the biconical phase. In addition, phase transitions near critical point are discussed. Results are compared to previous findings.

Index words: $3D$ Heisenberg Model, histogram reweighting, bicritical point, phase transition

Monte Carlo Study of Multicritical Behavior of the 3D Anisotropic Heisenberg Model

by

Siyan Hu

M.S., Shanghai University, Shanghai, China, 2007

A Thesis Submitted to the Graduate Faculty
of The University of Georgia in Partial Fulfillment
of the
Requirements for the Degree

Master of Science

Athens, Georgia

2011

Monte Carlo Study of Multicritical Behavior of the 3D Anisotropic Heisenberg Model

by

Siyan Hu

Approved:

Major Professor: David Landau

Committee: Michael Bachmann
Bernd Schuttler

Electronic Version Approved:

Maureen Grasso
Dean of the Graduate School
The University of Georgia
August 2011

Dedication

This paper is dedicated to my family. To be continued...

Acknowledgments

First and foremost, I'd like to express my sincere appreciation to my advisor, Professor Landau. I couldn't finish my research so smoothly and quickly without his insightful guidance and unlimited patience. He always gives me strong support and useful suggestions during my study.

I'd like to thank Dr Shan-ho Tsai. She helped me a lot whenever I met difficulties.

I'd like to thank Linda Lee and all CSP members, they all gave me an unforgettable graduate study during the past years.

Table of Contents

List of Figures

Chapter 1

Introduction

1.1 Background

There has been great interest in uniaxially anisotropic Heisenberg antiferromagnets in a magnetic field for many years. Most past studies focus on the phase diagram of the XXZ model. [1] Its Hamiltonian is described as:

$$\mathcal{H} = -J \sum_{i,j} [\Delta(S_i^x S_j^x + S_i^y S_j^y) + S_i^z S_j^z] - H \sum_i S_i^z \tag{1.1}$$

where J is the exchange coupling, i and j are neighboring sites on a simple cubic lattice. Δ is the uniaxial exchange anisotropy, $(0 < \Delta < 1)$. and H is the applied magnetic field along the $z-$axis. The phase diagram has been studied for many years, by using mean-field theory, [2] , renormalization group theory, [3] it is believed that an antiferromagnet (AF) phase (structure see below) exists at low temperature and low field. In addition, there are spin-flop (SF) and paramagnetic (P) phases. Phase transition boundaries of the paramagnetic (P) phase to the AF and SF phase are believed to be in the Ising universality class and XY universality classes, respectively. [4] There is a first order transition between the AF and SP phase and an bicritical end point is located where the three phase boundary lines meet.

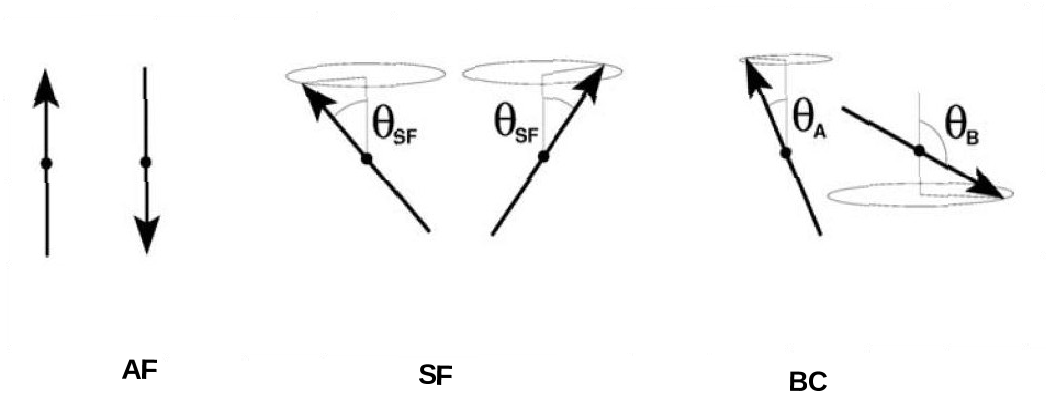

Figure 1.1: Spin Orientations on neighboring sites in the ground states of the XXZ models, corresponding to, from left to right, antiferromagnetic, spin-flop and biconical configurations. Arrows in each group represent spin configuration from two sublattices

However, it is argued that the bicritical point is unstable,that, instead, a tetracritical point exists, and that first order transition may be substituted with biconical(BC) structures near the vicinity of the meeting point of the three phases. [5] In the BC structures, both staggered z and xy will be nonzero while staggered z is zero in the SF phase and staggered xy is zero is AF phase. More details will be presented in the next section.

1.2 Model

Using Monte Carlo simulations, Selke (2011) obtained the phase diagram of the XXZ model on a simple cubic lattice in the vicinity of the AF-SF-P point [6] . At $\Delta = 0.8$, the

position of the meeting point is located at $k_BT/J = 1.025 \pm 0.015$ and $H/J = 3.9 \pm 0.03$ İn our thesis, we set $Delta = 0.8$ as well so that we make our results comparable with Selke(2011).

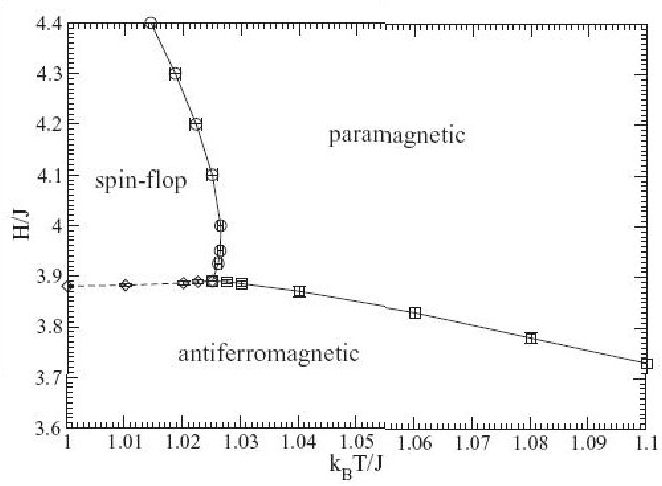

Figure 1.2: Phase diagram of the XXZ model on a simple cubic lattice in the vicinity of the AF-SF-P point. $\Delta = 0.8$, $J = -1$ [6]

As mentioned above, it has been noted recently [7] that a BC structure may also exist in the XXZ model, separating AF and SF phases. In the BC structure, spins from two sublattices A and B form different cones along the Z axis at different angles θ_A, θ_B. [1] See Figure 1.1.

However, the behavior of the BC structure is still controversial. It is uncertain if there is a BC structure bounded by second order phase lines or if we only have a single first order transition between AF and SF phase , See Figure 1.3(a). G.Bannasch *et al* (2009) believe there is a BC structure occurring at low temperatures close to the transition between the AF and SF phases. [4] See Figure 1.3(b). It is also argued a biconical structure may start at $T = 0$ and end at the AF-SF-P point. See Figure 1.3(c). Selke (2011) mapped the phase diagram by using Monte Carlo simulation and presented evidence for the meeting point of

AF-SF-P being a bicritical point by especially analyzing the Binder cumulant U^+_{xyz} and staggered susceptibility χ^+_{xyz} (definition see Chapter 4) at different lattice sizes $L = 8, 16, 24, 32$.

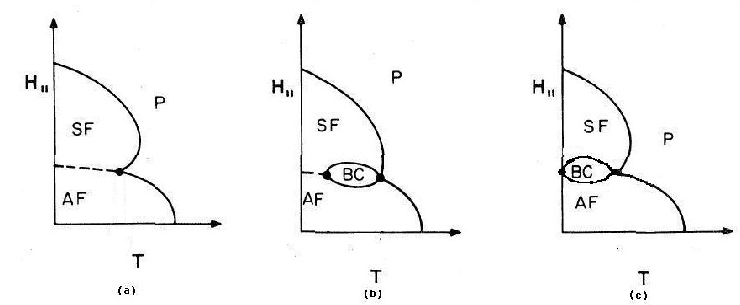

Figure 1.3: Possible phase diagrams in 3D Heisenberg XXZ model near multicritical region

In this thesis, we will use Monte Carlo simulation on the XXZ antiferromagnet on the simple cubic lattice to detect biconical structures near the multicritical point at around $T = 1.025$, according to Selke (2011), (See Figure 1.3, the meeting point of AF-SF-P phases) from another point of view. We will analyze different quantities related to the Ising, XY and Heisenberg order parameters to identify the meeting point of AF-SF-P. In particular, we consider larger lattice sizes, up to $L = 40$ and $L = 60$ in part, and more Monte Carlo steps for desired accuracy. Wolffcluster method is employed with standard Metropolis method. We also use histogram reweighting to analyze data near phase transition. Our goal is to seek any evidences of the existence of tetracritical point or bicritical point. In chapter 2, we introduce some background of Monte Carlo simulation. And in chapter 3, some useful theories of critical behavior are discussed. Chapter 4 is about the results we have got from our simulation and relevant discussion. Conclusion is presented in Chapter 5.

Chapter 2

Methods

2.1 Simple Sampling Monte Carlo Method

The average of some quantity A for each microstate of a system in thermodynamic equilibrium is given by:

$$< A >= \frac{1}{Z} \int A(x) e^{\frac{-\mathcal{H}(x)}{k_b T}} \, dx \tag{2.1}$$

where $A(x)$ is the quantity we are interested in, T is the temperature, k_b is the Boltzmann constant, $\mathcal{H}$ is the Hamiltonian. Z stands for the partition function given by:

$$Z = \int e^{\frac{-\mathcal{H}(x)}{k_b T}} \, dx \tag{2.2}$$

Hence, if the configurations space is discrete then the above two equations can be replaced with summing over all states as the following:

$$< A >= \frac{1}{Z} \sum_{all-states} A(x) e^{\frac{-\mathcal{H}(x)}{k_b T}} \tag{2.3}$$

In general, there are too many states to calculate $< A >$ exactly. To solve this problem, we usually select certain subsets of the total configuration space by using a random number generator to randomly produce spin states. This approach is called Monte Carlo method. Obviously, the simplest way to select sampled states is random points in phase space. It is known as *simple sampling* Monte Carlo method. Averages are then estimated by:

$$< A >_{appr.} = \frac{\sum_{n=1}^{N} A(x_n) e^{\frac{-\mathcal{H}(x_n)}{k_b T}}}{\sum_{n=1}^{N} e^{\frac{-\mathcal{H}(x_n)}{k_b T}}} \tag{2.4}$$

where N stands for the number of states.

From the above equation we can see that as $N \to \infty$, our estimation will be more and more accurate. [8]

However, simple sampling is appropriate for functions that are relatively smooth.(i.e. there are approximately equal probabilities in all of the states). Any sharp peak in the function might be missed by the simple sampling method. In order to solve this problem, we will introduce importance sampling.

2.2 Importance Sampling Monte Carlo Method

Importance sampling involves introducing a weight factor $\omega(x)$ to create a sampling density that varies as a function of x. [9] Then we get:

$$< A >= \int \omega(x) \frac{f(x)}{\omega(x)}\, dx. \tag{2.5}$$

If we change the variable to $dy = \omega(x)dx$ then it becomes:

$$< A >= \int \frac{f(x(y))}{\omega(x(y))}\, dy. \tag{2.6}$$

And it can be estimated by:

$$< A > \approx \frac{1}{N} \sum_{i=1}^{N} \frac{f(x(y_i))}{\omega(x(y_i))}. \tag{2.7}$$

As a result, we have f/ω over a uniform distribution in y rather than over a uniform distribution in x. The advantage to this is that ω can be chosen so that f/ω has a much lower variance than f. Thus we can weight the sampling of points towards their areas where f is changing the most. The result covers drawbacks of simple sampling and it gives rise to the name *importance sampling*.

In our case the importance sampling Monte Carlo method will yield the equation:

$$< A >_\beta \approx A(\bar{x})_\beta = \frac{[\sum_{i=1}^{N}[A(x(y_i))e^{-\beta\mathcal{H}(x(y_i))}/\omega(x(y_i))]}{\sum_{i=1}^{N}[e^{-\beta\mathcal{H}(x(y_i))}/\omega(x(y_i))]]} \tag{2.8}$$

where $\beta = 1/kT$ and again, N is the number of states sampled.

If we choose our $\omega(x) = P(x)$, where $P(x)$ is given by:

$$P(x) = \frac{1}{Z}e^{-\beta\mathcal{H}(x)}, \tag{2.9}$$

then it reduces to:

$$< A >_\beta = \frac{1}{N}\sum_{i=1}^{N} A(x(y_i)). \tag{2.10}$$

The Metropolis Algorithm [10] is used to choose the N states in order to get a sufficient distribution of the function $x(y)$. The next section is the introduction of the Metropolis Algorithm.

2.3 The Metropolis Algorithm

The principle of detailed balance is like the following [11] :

$$P(x_i)W(x_i \to x_j) = P(x_j)W(x_j \to x_i) \tag{2.11}$$

where $W(x_i \to x_j)$ is the transition rate from x_i to x_j in the phase space, and $P(x)$ is the probability of a certain state.

Hence, Equation 2.11 becomes:

$$P(x_j) = \frac{W(x_j \to x_i)}{W(x_i \to x_j)} = e^{-\Delta\mathcal{H}\beta} \tag{2.12}$$

$\Delta\mathcal{H}$ is the energy change $(\mathcal{H}(x_i) - \mathcal{H}(x_j))$. Any transition rate which satisfies detailed balance is acceptable. The first choice which was used in statistical physics is the Metropolis form. We will describe the Metropolis algorithm in the following recipe: [11]

1. Choose an initial state
2. choose a site i
3. Calculate the energy change $\Delta\mathcal{H}$ which results if the spin at site i is overturned
4. Generate a random number r such that $0 < r < 1$
5. If $r < e^{\frac{-\Delta\mathcal{H}}{kT}}$, flip the spin
6. Go the next site and go to (3)

After a set number of spins have been considered, the properties of the system are determined and added to the statistical average which is being kept. Note that the random number r is chosen $uniformly$ in the interval [0,1], and successive random numbers are uncorrelated. The accuracy of the result can also be improved by discarding the first D of the M steps. Normally, we will analyze the non-linear time-dependent correlation function to determine how much D we need to discard, which is described as:

$$\phi_A(t) = \frac{< A(t) - A(\infty) >}{< A(0) > - < A(\infty) >} \tag{2.13}$$

where $\phi_A(t)$ has an exponential decay at long time. [11] and the decay constant tells us how big D should be.

If D is large enough this will effectively eliminate the bias that results from the choice of the starting point x_0. The first D Monte Carlo Steps is referred to as *initialization* Monte

Carlo Steps and the next $M' = M - D$ MCS is referred as the *sampling* Monte Carlo steps. We still need to carefully choose how big M' is enough for the simulation based on the correlation function. Since too few samples will lead to a biased result while too many samples are good but time-consuming.

We can also use Equation 2.14 to describe the equilibrium correlation function in order to determine how many steps we need to discard among the successive Monte Carlo steps for independent samples:

$$\phi_{AA}(t) = \frac{< A(0)A(t) > - < A >^2}{< A^2 > - < A >^2} \tag{2.14}$$

It is worth mentioning that although the above receipe involve the Ising model, we still apply the algorithm to Heisenberg Model with rotating the spin with some random angle instead of overturning it.

2.4 Histogram Reweighting

Monte Carlo simulations have been used for many years to study the properties of physical models. A major concern for any thorough and accurate MC study is the amount of computer resources required. For large scale computations, such as those necessary to study lattice gauge theories, the power and efficiency of the simulation are of major importance. Hence, Ferrenberg *et al* [12] proposed a different, but complementary, approach to improving efficiency is to increase the amount of information obtained from a simulation. The data usually obtained from a MC simulation are averages of thermodynamic quantities at the single point in parameter space for which the simulation is performed. The technique uses multiple restricted-energy MC simulations to generate the partition function for a range of parameter values.

Consider the Ising model in a magnetic field. The Hamiltonian for this system is:

$$-\beta\mathcal{H} = K\sum_{<i,j>}\sigma_i\sigma_j + h\sum_i \sigma_i = KS + hM \tag{2.15}$$

where K is the dimensionless coupling constant (J/kT) and h is an applied magnetic field (H/kT). The probability distribution of S and M at a point in the parameter space(K, h) is given by:

$$P_{K,h}(S, M) = \frac{1}{Z(K, h)}N(S, M)exp(KS + hM) \tag{2.16}$$

where $N(S, M)$ is the number of configurations at the point (S, M) in the configurations at the point (S, M) in the phase space, and $Z(K, h)$ is the canonical partition function given by:

$$Z(K, h) = \sum_{S,M} N(S, M)exp(KS + hM). \tag{2.17}$$

The normalized probability distribution with new parameters (K', h') can be described in terms of (K, h) in the following way:

$$P_{K',h'}(S, M) = \frac{P_{K,h}(S, M)exp[(K' - K)S + (h' - h)M]}{\sum_{S,M} P_{(K,h)}(S, M)exp[(K' - k)S + (h' - h)M]} \tag{2.18}$$

Using this reweighted probability distribution $P(S', M')$, we can calculate new thermodynamic quantities based on the data given from (S, M).

2.5 Fluctuations

We are often interested in macroscopic properties of the system being studied, including specific heat, susceptibility, etc. Typically, the system is held at a fixed temperature. And such quantities are allowed to fluctuate about their equilibrium values. $\beta \equiv \frac{1}{kT}$, as we defined before, U is the fluctuating internal energy and $\bar{U}$ is the average energy.
We will have: [11]

$$\begin{aligned} \bar{U}(\beta) &= <\mathcal{H}(\mu)> \\ &\equiv \frac{\sum_\mu \mathcal{H}(\mu) e^{-\beta\mathcal{H}(\mu)}}{\sum_\mu e^{-\beta\mathcal{H}(\mu)}} \\ &= \sum_\mu P_\mu \mathcal{H}(\mu) \end{aligned} \tag{2.19}$$

while $<\mathcal{H}^2>$ is denoted as:

$$<\mathcal{H}^2> = \frac{\sum_\mu \mathcal{H}^2 e^{-\beta\mathcal{H}(\mu)}}{\sum_\mu e^{-\beta\mathcal{H}(\mu)}} \tag{2.20}$$

Note that the relation:

$$-(\frac{\partial U(\beta)}{\partial \beta})_V = <\mathcal{H}^2> - <\mathcal{H}>^2 . \tag{2.21}$$

And since $(\partial U/\partial T)_V = C_V$, the specific heat thus yields a fluctuation relation:

$$\begin{aligned} k_B T^2 C_V &= <\mathcal{H}^2> - <\mathcal{H}>^2 \\ &= <(\Delta U)^2>_{NVT}, \end{aligned} \tag{2.22}$$

where $\Delta U \equiv \mathcal{H} - <\mathcal{H}>$.

2.6 Finite Size Scaling

Often, we find it is hard to distinguish between first order and second order transitions since thermodynamic properties for finite systems are smooth as they pass through a phase transition. So it is important to use the finite size scaling to distinguish these two types of transitions, [13] also to locate transitions, determine critical behavior, etc.

At a second order transition, the critical behavior of a system in the thermodynamic limit can be extracted from the size dependence of the singular part of the free energy, which, according to finite size scaling theory, is described by a scaling ansatz similar to the

scaling of the free energy with thermodynamic variables T, H. [14] We can deduce different thermodynamic properties based on the differentiation of the free energy:

$$M = L^{-\beta/\nu} M^0(\epsilon L^{1/\nu}) \tag{2.23}$$

$$\chi = L^{\gamma/\nu} \chi^0(\epsilon L^{1/\nu}) \tag{2.24}$$

$$C = L^{\alpha/\nu} C^0(\epsilon L^{1/\nu}) \tag{2.25}$$

where M, χ and C stand for magnetization, susceptibility and specific heat, respectively. $M^0(x), \chi^0(x)$ and $C^0(x)$ are their corresponding scaling functions. However, since the finite size scaling ansatz is only valid for sufficiently large size, we need some correction terms when it is in smaller systems or at temperatures away from T_c. (We are not going to discuss too much details here) See Liu and fisher (1990), Ferrenberg and Landau (1991). The scaling functions $M^0(x), C^0(x), \chi^0(x)$ will reduce to proportionality constants as the following:

$$M \propto L^{-\beta/\nu} \tag{2.26}$$

$$\chi \propto L^{\gamma/\nu} \tag{2.27}$$

$$C \propto L^{\alpha/\nu} \tag{2.28}$$

α, β, γ, ν are all critical exponents which are identical in the same universality class. Equations 2.26 $\sim$ 2.28 can be used to extract estimates for the ratio of certain critical exponents.

Another way to determine the transition temperature accurately is to locate the peaks in the thermodynamic derivatives. We can write:

$$T_c(L) = T_c + \lambda L^{-1/\nu}(1 + bL^{-\varpi}) \tag{2.29}$$

$$K_c(L) = K_c + \lambda' L^{-1/\nu}(1 + b'L^{-\varpi}) \tag{2.30}$$

where b, λ' , b' are constants. Each thermodynamic quantity has its own scaling function while the peaks occur at different temperatures for finite systems. We can use the above equations to locate the infinite lattice transition. Of course, it requires very good statistical accuracy because we should have all K_c, ν, ϖ the same for all properties.

$$\frac{\partial ln < m^n >}{\partial K} = (< m^n E > / < m^n >) - < E > . \tag{2.31}$$

For different nth power of cumulant, they share the same slope. Hence, the location of the maxima in these quantities also provides us with estimates for $K_c(L)$ which can be used in extrapolate K_c.

Chapter 3

Critical Behavior and Multicritical Behavior

3.1 Introduction

Different systems may undergo a variety of phase transitions and phase diagrams can be drawn to show the boundaries between these phases. For the phase diagram, the critical point is known as the location in the equilibrium phase diagram where a first order line representing the boundary between two phases terminate. When system comes close to the critical point, it will show various singular properties, for instance, the magnetic susceptibility, the heat capacity will diverge at the critical point.

3.2 Phase Transitions

A phase is a set of states for a system where the general physical properties are relatively uniform. Common phases include gases, liquids, solids, ferromagnets, antiferromagnets, etc.

It has been proved that the densities of the thermodynamic potentials may exhibit singularities in the thermodynamic limit. The singular points determine the *phase diagram* of the system and the singularities are interpreted as changes in the phase structure of the system, i.e. as *phase transitions*.

There are two main types of phase transitions, first-order and second-order.

A first-order phase transition is defined as having a discontinuities of the first derivatives of free energy while the second order phase transition has discontinuity of the second derivatives but the first derivatives are continuous. [8] A body-centered cubic

nearest-neighbor ferromagnet in zero field is an example of a system with a second-order phase transition. Also, a typical first order transition is ice undergoing melting. When ice melts, the temperature remains constant while the entropy is discontinuous. [15] A line of first order phase transitions is called a *coexistence line*, since two different phases can coexist on it, and such a line will terminate at an "end-point" called a *critical point*. Hence, the critical point is a point in the space of thermodynamic variables at which the differences between two coexisting phases disappear. [16]

3.3 Order Parameter

The order parameter is a distinguishing feature of most phase transitions, which will appear as a non-zero value in the ordered phase but is zero in the disordered phase. [11] Order parameters can be different in all kinds of physical systems. For instance, the magnetization is the order parameter for an ferromagnetic Ising model, and the difference in the density between the liquid and gas phases is the order parameter in a liquid-gas system.

3.4 Critical Exponents

Our interest is to study the thermodynamic behavior near the critical region. We usually focus on the reduced temperature instead of the absolute temperature. The reduced temperature is a measure of the distance from the critical temperature T_c, as the following:

$$\epsilon \;=\; |1 - \frac{T}{T_c}|. \tag{3.1}$$

Some thermodynamic properties can be expressed in terms of the reduced temperature by power laws near the critical point T_c

$$\chi = \chi_0 \epsilon^{-\gamma} \tag{3.2}$$

$$C = C_0 \epsilon^{-\alpha} \tag{3.3}$$

$$\xi = \xi_0 \epsilon^{-\nu} \tag{3.4}$$

$$m = m_0 \epsilon^{\beta} \tag{3.5}$$

$\gamma, \alpha, \nu, \beta$ are all critical exponents and χ_0, C_0, ξ_0, m_0 are critical amplitudes. The above four equations are only valid as $\epsilon \to 0$, so correction to scaling terms might be needed to correct the deviations from asymptotic behavior. [4]

A multicritical point is an intersection point of multiple curves of second order transitions, whose thermodynamic properties still obey the power law relations, and the values of exponents can be determined from different multicritical universality classes.

3.5 Universality

The principle of universality can be defined as the following: Depending on the dimensionality and the symmetry, we can have different systems having identical behavior in the critical region. Hence, they have identical critical exponents for these systems. In that case, we say these systems belong to the same universality class. [11] Other properties can also determine the universality class such as the spatial dimensionality, spin dimensionality, symmetry of the ordered state, the presence of symmetry breaking fields and the range of interactions. [15] The principle of universality is a powerful tool since we can simulate "real" system as a "simple" system in the same universality class. The behavior of the simple system will match that of the complicated system when both are close to the critical point.

Chapter 4

Results

4.1 Background

We will focus our study on the XXZ Heisenberg Antiferromagnet in a magnetic field on the simple cubic lattice. Its Hamiltonian describing it is written as the following:

$$\mathcal{H} = -J\sum_{i,j}[\Delta(S_i^x S_j^x + S_i^y S_j^y) + S_i^z S_j^z] - H\sum_i S_i^z \tag{4.1}$$

where J is the exchange coupling and $J > 0$. i, j stands for the spins at neighboring sites in the lattice and Δ is the uniaxial exchange anisotropy. In our thesis, $\Delta = 0.8$. H is the applied external magnetic field along the z-axis. We use the standard Metropolis Monte Carlo algorithm and Wolffcluster method, also a simple cubic lattice with periodic boundary conditions is employed. We study the lattice sizes $L = 10, 20, 30, 40$ while error bars are estimated by averaging over at least three independent runs. In order to get reliable statistics, large number of independent measurements is necessary. Also large enough system sizes are needed due to finite size effect. Limited by the computer resources and time, we choose the histogram method to provide an efficient way to extract thermodynamic information near the temperatures that we actually run. Generally, we take 10^6 hybrid steps for $L = 10$, 2×10^6 for $L = 20$, 3×10^6 for $L = 30$ and 4×10^6 for $L = 40$. In particular, for the points where we take for the reweighting, we collect more Monte Carlo samples, specifically 5×10^6 for $L = 20$, 6×10^6 for $L = 30$, 1.2×10^7 for $L = 40$ and for $L = 60$ at $T = 1.025$, we collect 1.5×10^7 samples to do reweighting. It is worthing mentioning that for each hybrid step, we run 6 Wolffcluster and 4 Metropolis steps.

To map the phase diagram, we carefully pick out the quantities that are relevant to the Ising, XY and Heisenberg order parameters. In particular, we choose the staggered z magnetization and staggered xy magnetization quantities as interest. Staggered magnetization M_α^+ is the magnetization (α stand for z, xy, etc) from sublattice A minus the magnetization from sublattice B. The reason is when it comes into the SP phase from AF phase, the staggered magnetization z will decrease from 1 to 0 which indicates the phase transition. And the stggered magnetization xy will also change from 0 in the AF phase to large values in SP phase. These two quantities will be sufficient for us to identify the phase transition. We calculate the corresponding staggered susceptibility χ_z^+, χ_{xy}^+ and Binder fourth order cumulants U_z^+, U_{xy}^+ as the following:

$$\chi_z^+ = \frac{< M_z^{+2} > - < M_z^+ >^2}{kT} \tag{4.2}$$

$$\chi_{xy}^+ = \frac{< M_{xy}^{+2} > - < M_{xy}^+ >^2}{kT} \tag{4.3}$$

$$U_z^+ = 1 - \frac{< M_z^{+4} >}{3 < M_z^{+2} >^2} \tag{4.4}$$

$$U_{xy}^+ = 1 - \frac{< M_{xy}^{+4} >}{3 < M_{xy}^{+2} >^2} \tag{4.5}$$

Selke(2011) used staggered susceptibility χ_{xyz}^+ and cumulant U_{xyz}^+ to identify a bicritical point with Heisenberg symmetry, which are defined as:

$$\chi_{xyz}^+ = \frac{< M_{xyz}^{+2} > - < M_{xyz}^+ >^2}{kT} \tag{4.6}$$

$$U_{xyz}^+ = 1 - \frac{< M_{xyz}^{+4} >}{3 < M_{xyz}^{+2} >^2} \tag{4.7}$$

$$\tag{4.8}$$

4.2 Results for T = 0.95

We start our study at fixed temperature $T = 0.95$, and sweep the field. We change our lattice size from $L = 10$ to $L = 40$. According to Selke(2011), at low temperatures, if the

external field is low enough (see Figure 1.2), the system is in the antiferromagnetic state and will turn into spin-flop phase if the external field increases. The transition between AF and SF phases is believed to be the first order transition only if there is no biconical phase. As found in our Monte Carlo runs, Figure 4.1, 4.2 below show the behavior of both order parameters when field changes. It indicates that the order parameter M_z^+ on different lattice sizes starts from zero at low field, and is nonzero in the AF phase and may gradually go to 0 in the SP phase. The position where the highest slope occurs indicates the transition location. As we can see from Figure 4.1 and 4.2, the curve gets sharper and sharper as the lattice size goes up, and when $L = 40$, we have the largest slope around $H=$ $3.835 \sim 3.84$, which indicates the transition occurs in that region.

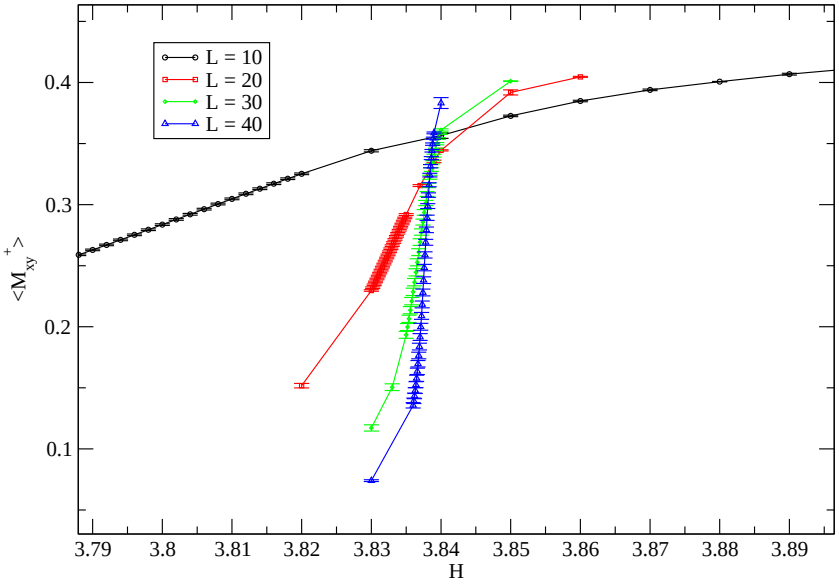

Figure 4.1: Order Parameter M_{xy}^+ for $T = 0.95$, $\Delta = 0.8$

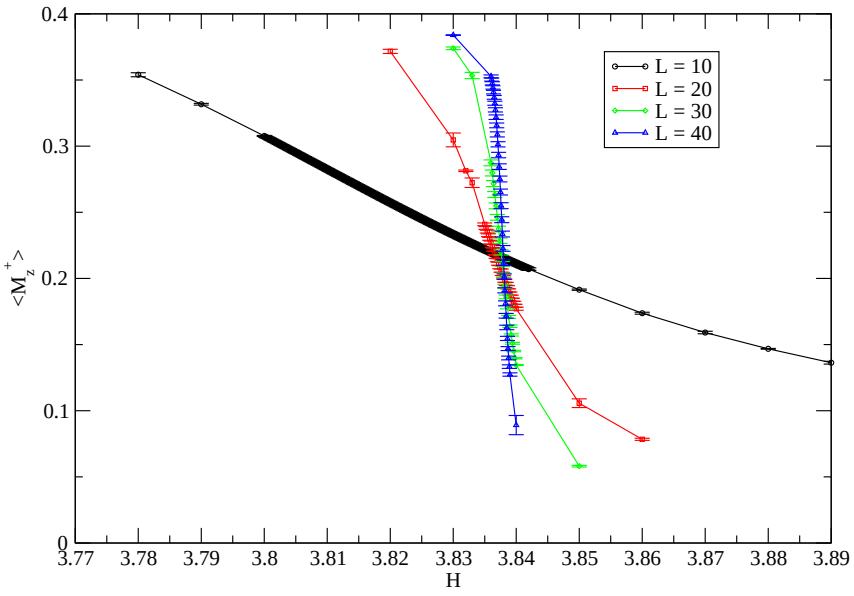

Figure 4.2: Order Parameter M_z^+ for $T = 0.95$, $\Delta = 0.8$

Figure 4.3 and 4.4 show the susceptibilities of the two order parameters respectively. The location of the curves' peaks indicate the phase transitions, from which we can tell the peak of χ_{xy}^+ shifts toward right hand side as the lattice size increases. And at $L = 40$ the highest susceptibility is located at H between 3.8374 and 3.8378 within error bars. Also, the peak of χ_z^+ moves toward right and when $L = 40$, the peak is within 3.8377 and 3.8382. The movement of the peak is due to the finite size effect and from Figure 4.1 $\sim$ 4.4, we are confident that the susceptibility peaks of both χ_z^+ and χ_{xy}^+ occur at about the same H within error bars. Hence, it provides an indication of only one transition at $T = 0.95$, and we don't have evidence at this temperature to suggest that we have two phase transitions that would be expected if there was a biconical structure.

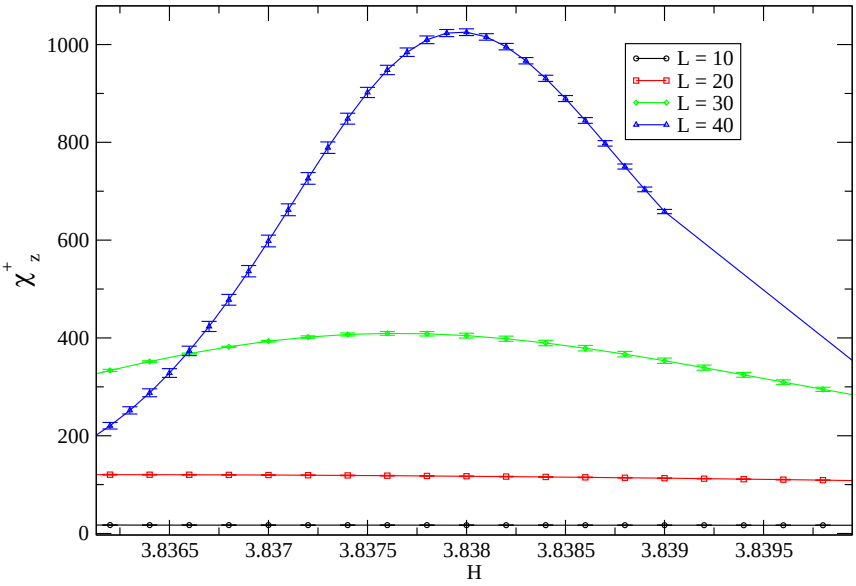

Figure 4.3: Susceptibility χ_z^+ for $T = 0.95$, $\Delta = 0.8$

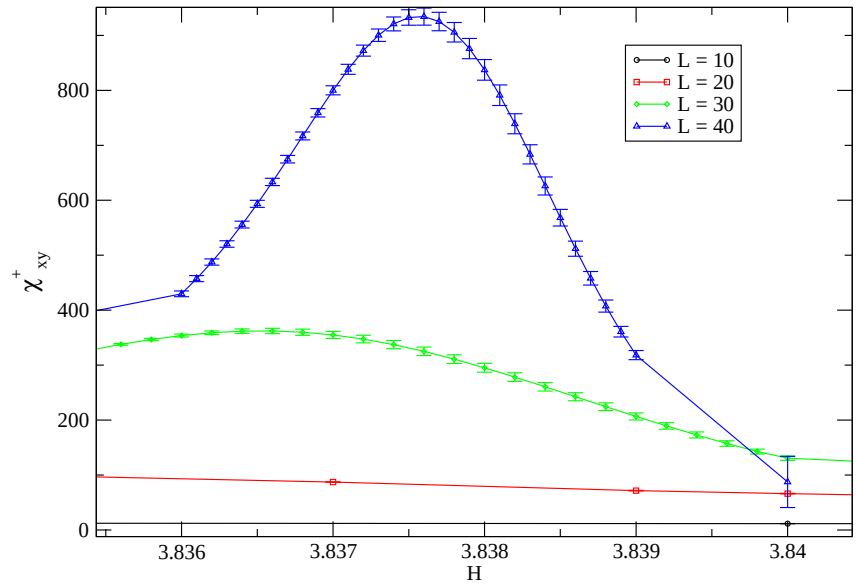

Figure 4.4: Susceptibility χ_{xy}^+ for $T = 0.95$, $\Delta = 0.8$

We check the cumulant of U_{xy}^{+} and U_{z}^{+}. Figure 4.5 indicates the crossover point shifts towards the right hand side as the lattice size gets larger, because of the finite size effect. The two largest lattice sizes, $L = 30$ and $L = 40$ intersect for H at $3.8382 \sim 3.8383$. If we look at the cumulant U_{xy}^{+} versus field plot at Figure 4.6, the crossing point is also between $3.8382 \sim 3.8383$. This demonstrates that both order parameters' cumulants cross at the same external field, and thus indicates there is only one transition at this temperature. It is worth mentioning if we have a biconical structure at $T = 0.95$, we will expect to see susceptibility peaks of χ_{xy}^{+} and χ_{z}^{+} are at different H and cumulant crossing points of U_{xy}^{+} and U_{z}^{+} are also at different H, because M_{z}^{+} will be zero at the upper bound of biconical structure and M_{xy}^{+} will be zero at lower bound of biconical structure. However, Figure 4.1 $\sim$ 4.6 indicate the phase transition occurs at the same H within error bars, we can only conclude we have a first order transition at $T = 0.95$.

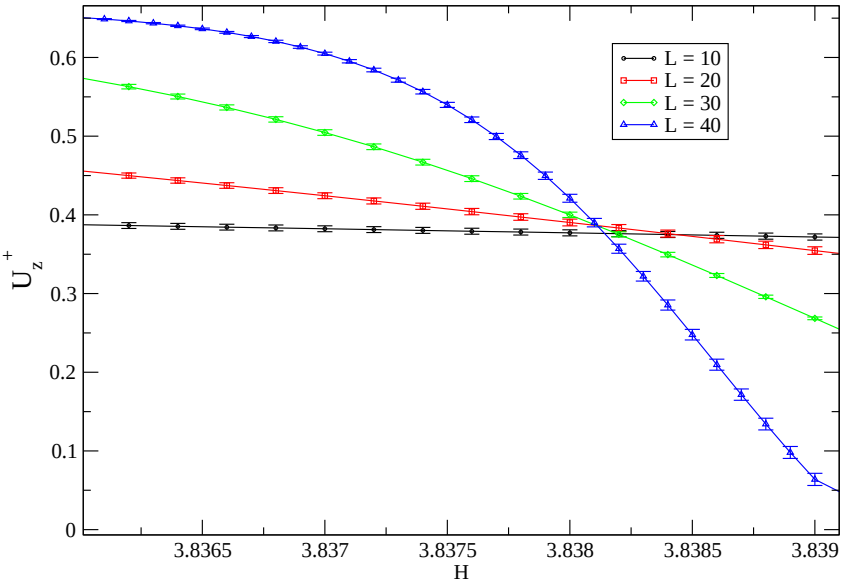

Figure 4.5: Cumulant U_{z}^{+} for $T = 0.95$, $\Delta = 0.8$

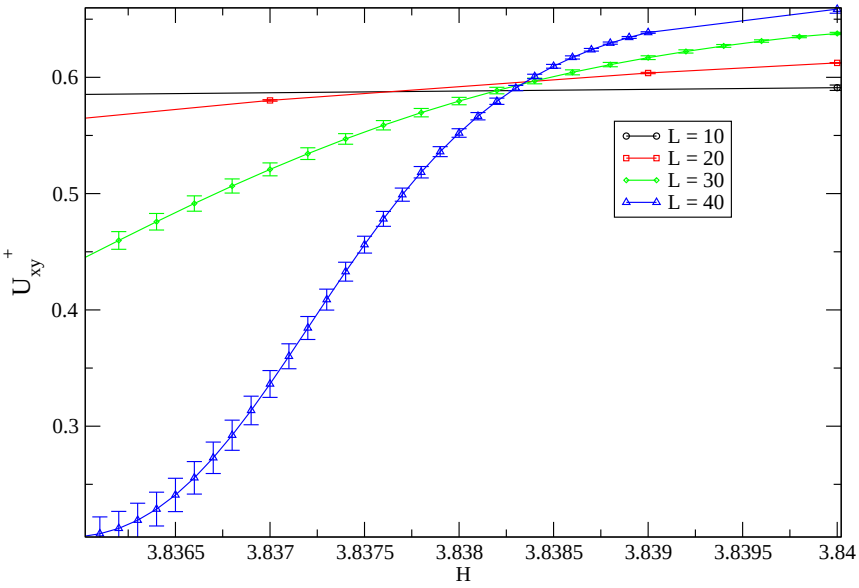

Figure 4.6: Cumulant U_{xy}^{+} for $T = 0.95$, $\Delta = 0.8$

We show a log-log plot of the finite size scaling in Figure 4.7. We do a linear regression on all four data points and get a slope nearly equal to 3. We know the first order transition goes with L^d, where $d = 3$ is the dimension of our model, and the finite size scaling fit in Figure 4.7 is consistent with the first order behavior. We conclude at $T = 0.95$, there is only a first order transition between AP and SP phases and no indication of a biconical phase bounded by two second order phase boundaries.

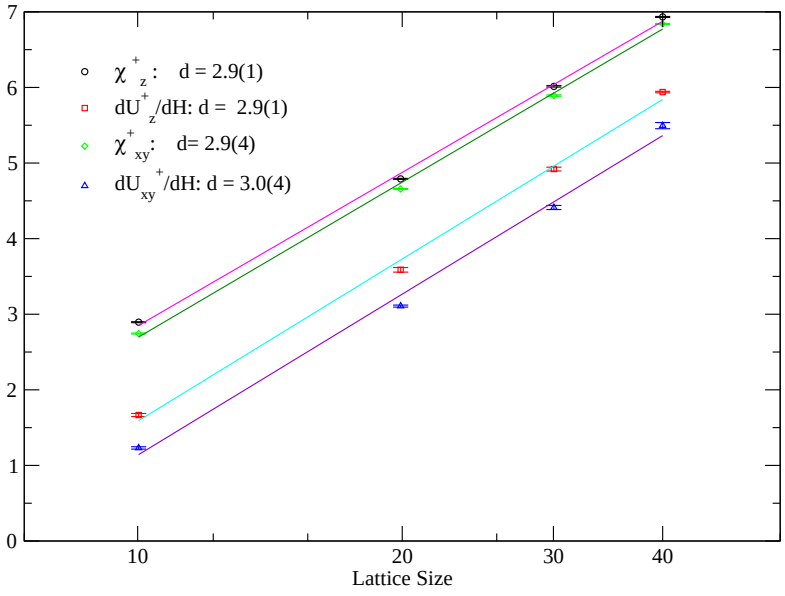

Figure 4.7: Finite Size Scaling for $T = 0.95$, the straight lines are fitted lines from data points

4.3 Results for T = 0.98

We move to a higher temperature at $T = 0.98$ and sweep the external field to analyze these quantities. The largest slopes of both M_z^+ and M_{xy}^+ occur at about $H = 3.86$. The susceptibility of χ_{xy}^+ and χ_z^+ show the largest peaks locate around $3.860 \sim 3.861$ within error bars. Also the cumulants of U_{xy}^+ and U_z^+ cross between 3.861∼3.8615. All the evidences show we have one transition at $H = 3.86 \sim 3.8615$ at $T = 0.98$, and we fail to see any biconical phase existing so far.

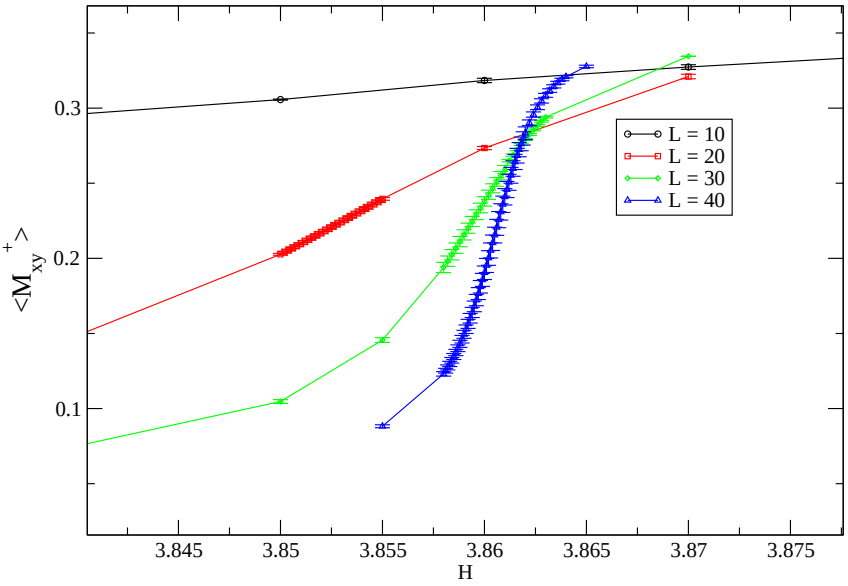

Figure 4.8: Order Parameter M_{xy}^{+} for $T = 0.98$, $\Delta = 0.8$

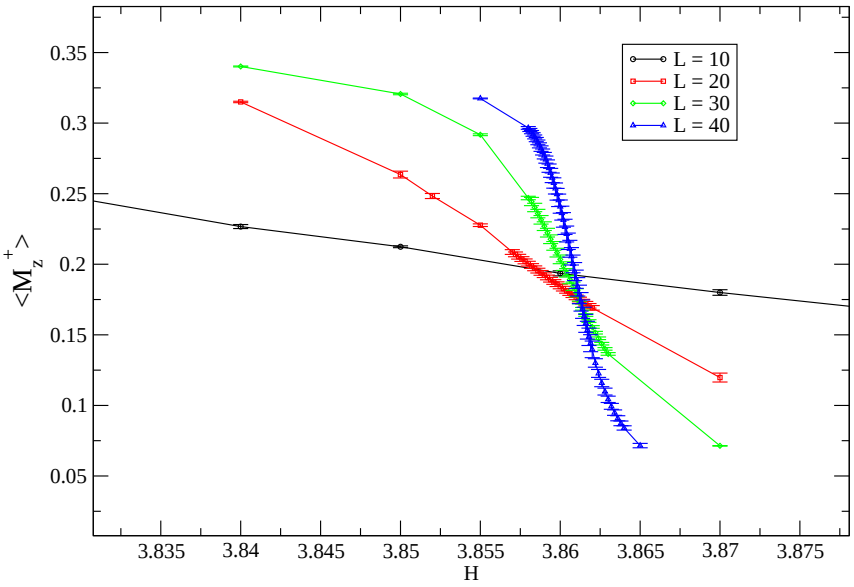

Figure 4.9: Order Parameter M_{z}^{+} for $T = 0.98$, $\Delta = 0.8$

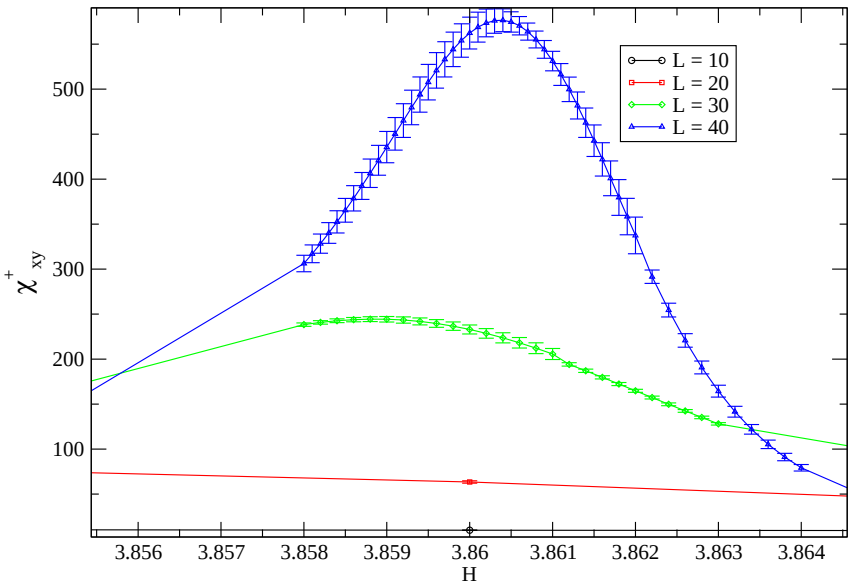

Figure 4.10: Susceptibility χ^+_{xy} for $T = 0.98$, $\Delta = 0.8$

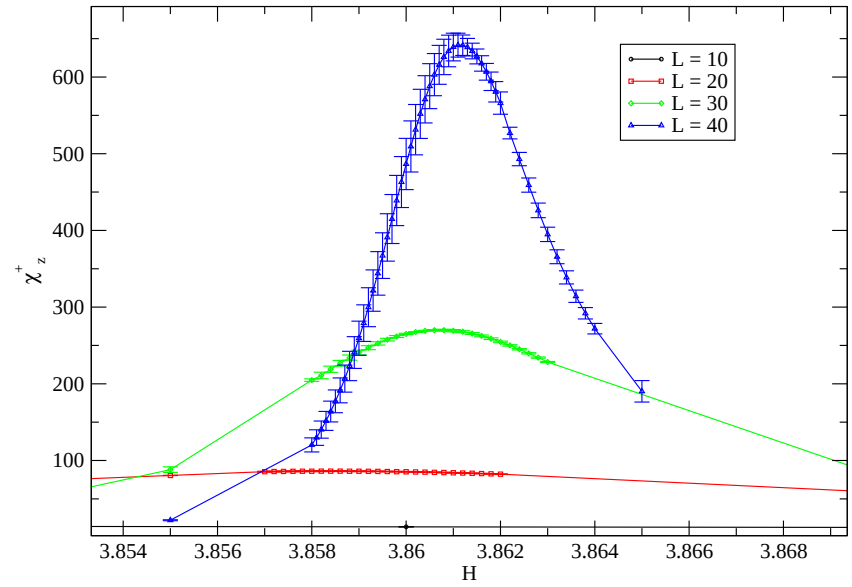

Figure 4.11: Susceptibility χ^+_z for $T = 0.98$, $\Delta = 0.8$

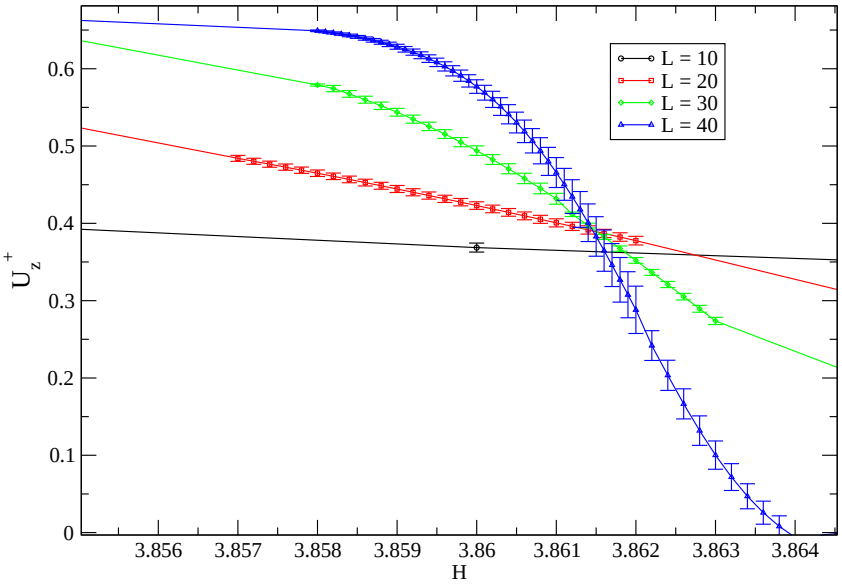

Figure 4.12: Cumulant U_z^+ for $T = 0.98$, $\Delta = 0.8$

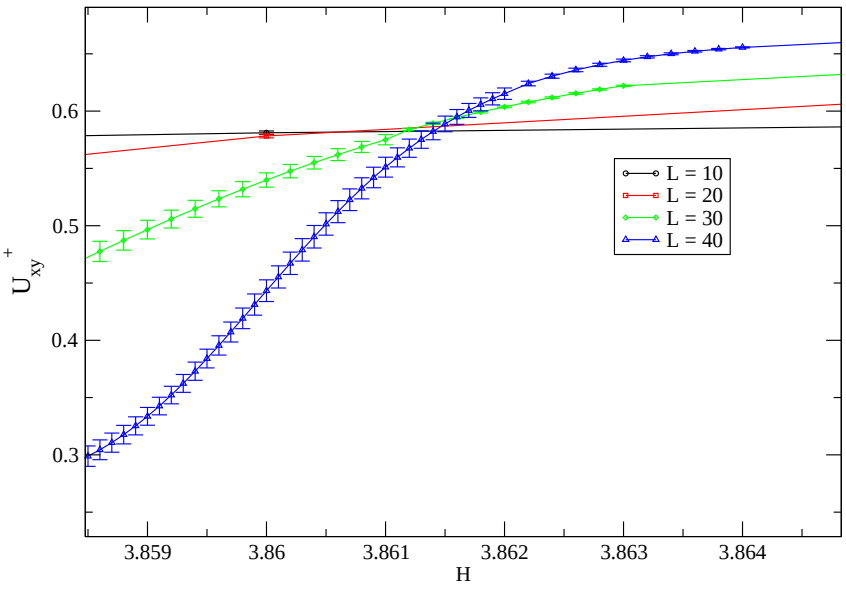

Figure 4.13: Cumulant U_{xy}^+ for $T = 0.98$, $\Delta = 0.8$

Also, if we look at the finite size scaling plot for the maxima, the slope is less than 3 if we fit four lattice sizes, namely $L = 10$, 20, 30, and 40. However, because $T = 0.98$ is close to the multicritical point, we may have crossover effects and finite-size effects become stronger. Therefore, the first-order nature of the transition is only evident when large lattice sizes are considered. In fact, if we use $L = 10$ to $L = 40$ to fit the line, the exponent is no longer 3; however, if we only use the two larger system sizes in the fitting ($L = 30$ and 40), then the slope increases and its value is close to 3. (d, *i.e.* slope shown in Figure 4.14 is from linear fittings using the two larger L in each case.) This means we still have a first order transition at $T = 0.98$, but because the finite-size effects are much stronger, our analyses cannot include data for the smaller lattice sizes. This means we still have a first order transition here, but it is no longer as clear as what we have at $T = 0.95$.

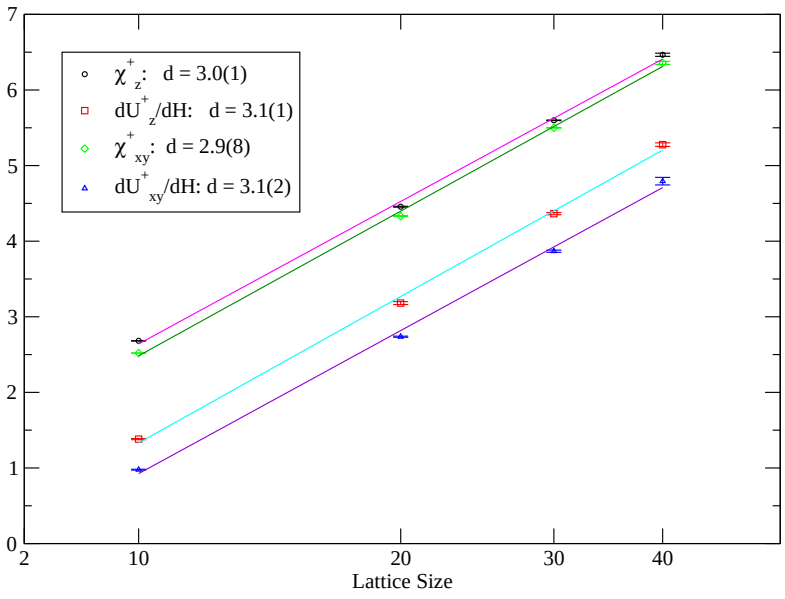

Figure 4.14: Finite Size Scaling for $T = 0.98$, the d shown in the graph are the slopes from fitting the largest two sizes $L = 30$, $L = 40$

4.4 Results for T = 1.01

We take a look at T = 1.01, which is even closer to the multiricitical point $T = 1.025$. In Figure 4.15 and 4.16, the order parameters data for M_z^+ and M_{xy}^+ both demonstrate the biggest slope at around $H = 3.883 \sim 3.885$. Susceptibilities for χ_z^+ and χ_{xy}^+ locate the peaks between 3.883 and 3.885 within error bars. The crossing points of the cumulant for U_z^+ and U_{xy}^+ also stay around $H = 3.886$. Finite size scaling plot in Figure 4.21 indicates the exponent is away from 3 in contrast to lower temperatures. However, due to the crossover effect, if we only fit the last two lattice sizes $L = 30$ and $L = 40$ to a power law, we will have larger slope, and it is believed if we run larger lattice size, the exponent will get closer and closer to 3 due to the stronger asymptotic behavior. Since $T = 1.01$ is quite close to the multicritical point, the crossover effect is dominant, hence the indication of the first order transition is even weaker than lower temperatures.

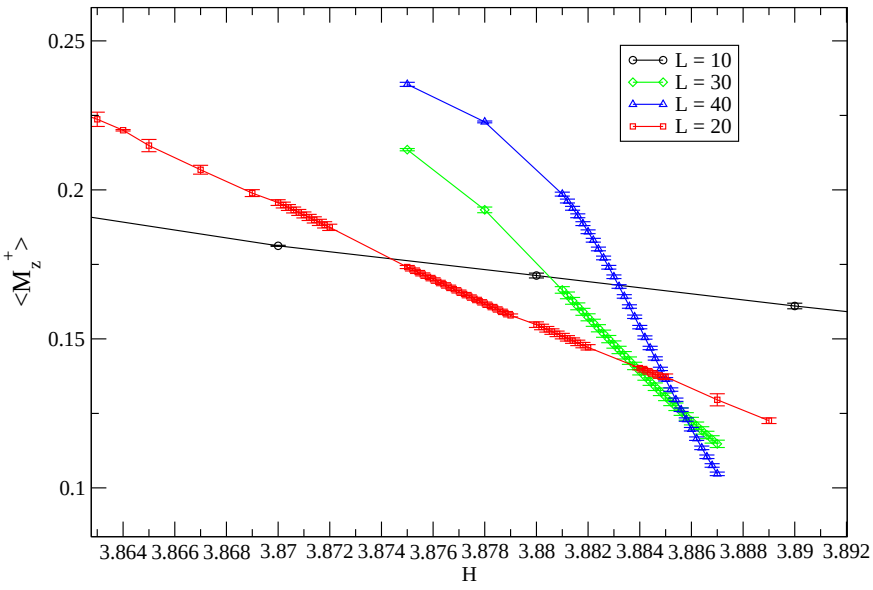

Figure 4.15: Order Parameter M_z^+ for $T = 1.01$, $\Delta = 0.8$

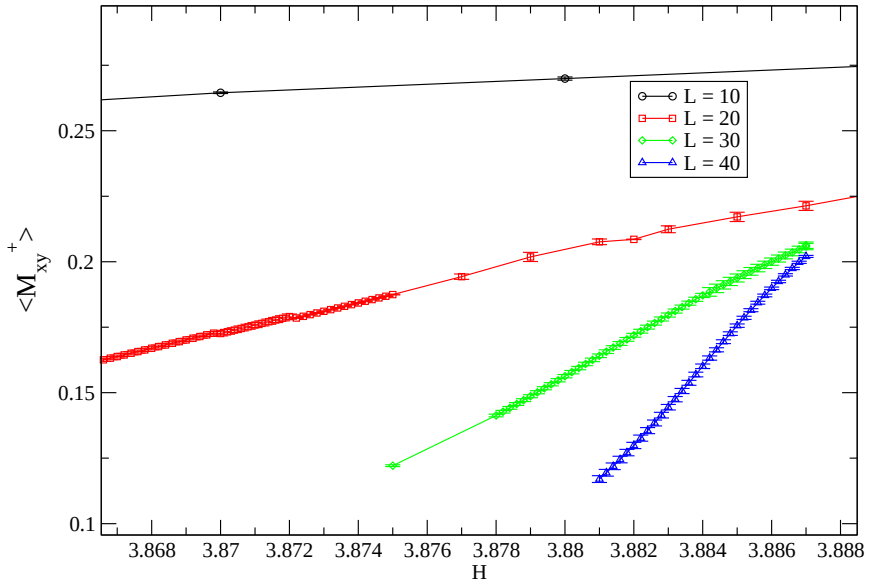

Figure 4.16: Order Parameter M_{xy}^{+} for $T = 1.01$, $\Delta = 0.8$

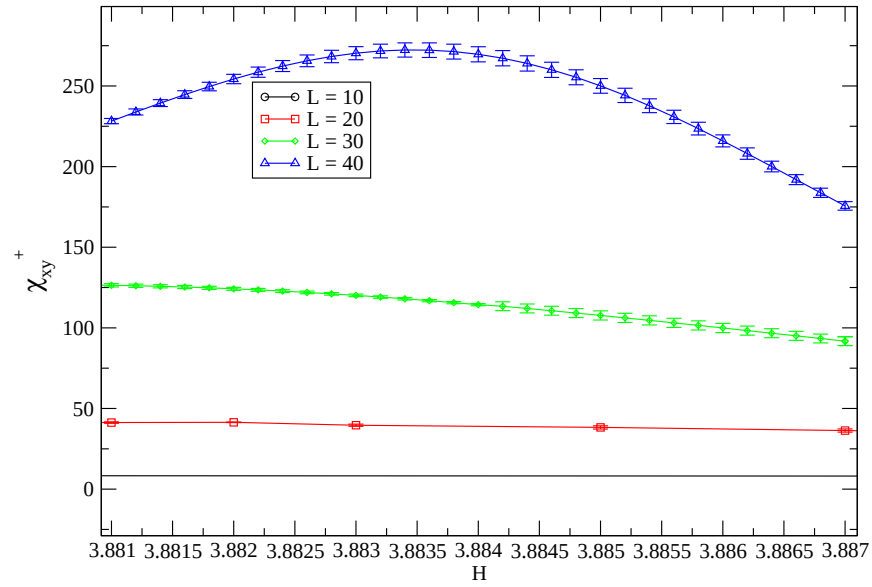

Figure 4.17: Susceptibility χ_{xy}^{+} for $T = 1.01$, $\Delta = 0.8$

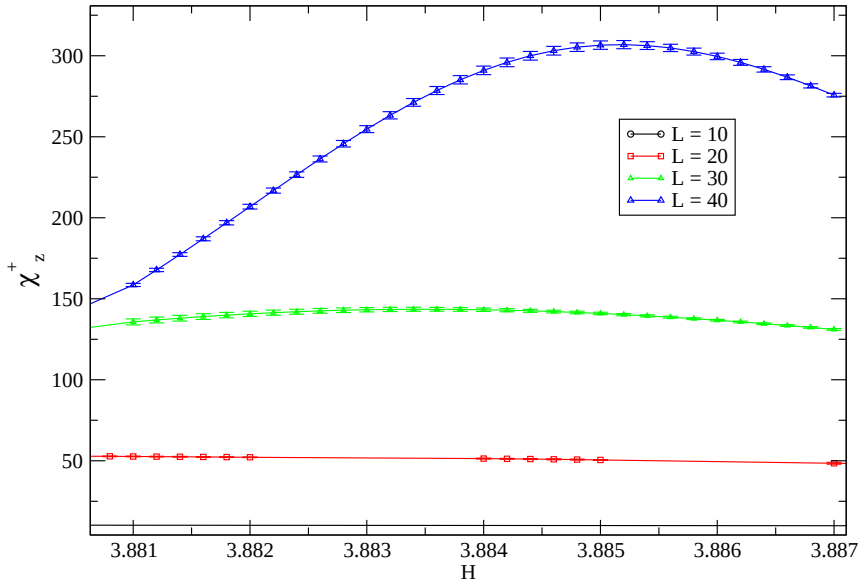

Figure 4.18: Susceptibility χ_z^+ for $T = 1.01$, $\Delta = 0.8$

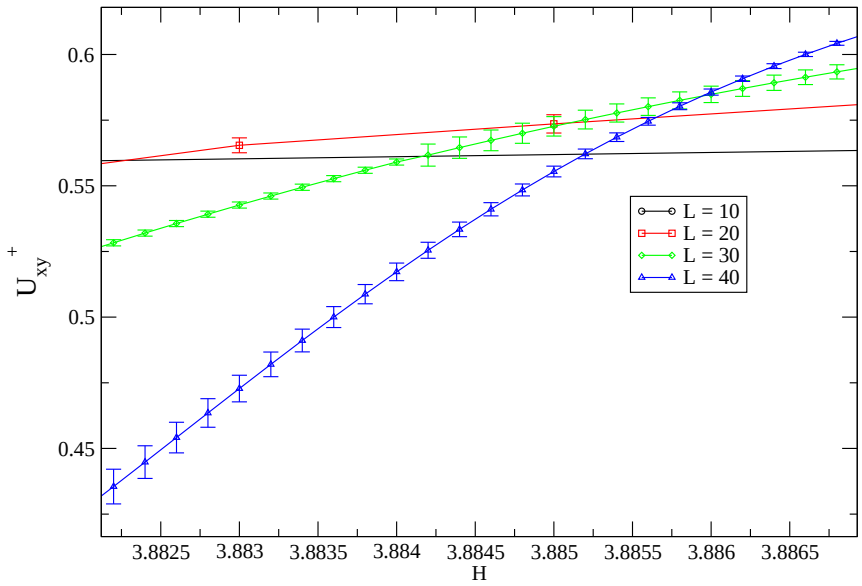

Figure 4.19: Cumulant U_{xy}^+ for $T = 1.01$, $\Delta = 0.8$

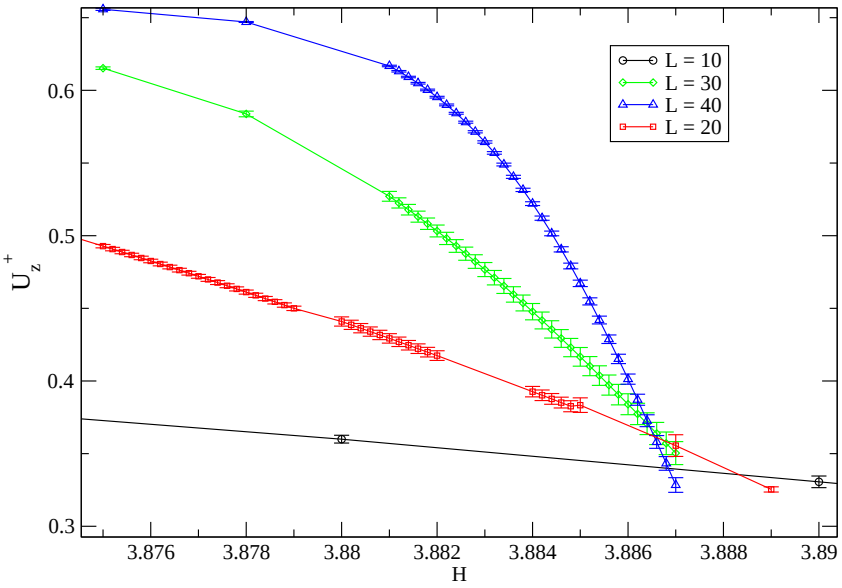

Figure 4.20: Cumulant U_z^+ for $T = 1.01$, $\Delta = 0.8$

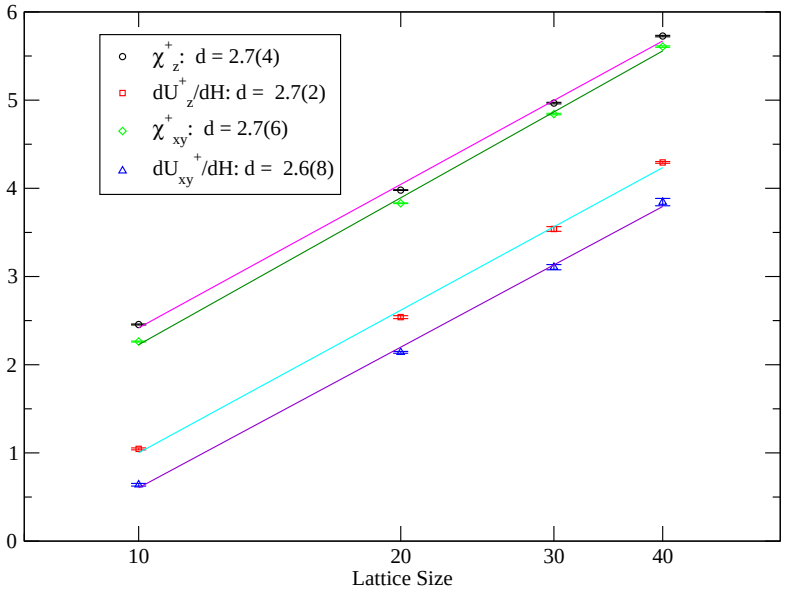

Figure 4.21: Finite Size Scaling for $T = 1.01$, the d shown in the graph are the slopes from fitting the largest two sizes $L = 30$, $L = 40$

4.5 Results for T =1.025

In this section, we do the analysis for $T = 1.025$, which, according to the Selke (2011), is the bicritical point location ($T = 1.025 \pm 0.015$) and belongs to the $3D$ Heisenberg universality class. By looking at the order parameters of M_z^+ and M_{xy}^+, we confirm the transition may occur between the field $H = 3.892 \sim 3.896$. Our susceptibility data also locates the peaks at $H = 3.890 \sim 3.897$. Cumulant curves intersect at about $H = 3.899$. Since it is almost at the multicritical point, we will have critical slowing down at phase transitions, which happens when the temperature T approaches to critical point T_c, we will have longer correlation times, hence more Monte Carlo steps need to be run in order to get accurate results. We collect at least 10^7 samples for larger sizes and L ranges from 10 to 60 in order to locate the transition point precisely.

We show a log-log plot of the finite size scaling and analysis the critical exponents. We have the following relationship:

$$\chi \sim L^{\frac{\gamma}{\nu}}$$

and the theoretical value for $3D$ Heisenberg universality class is $\gamma = 1.37(5)$ and $\nu = 0.70(5)$ respectively [17] . Hence, if we do the log-log plot and the slope of the regression line will be $\frac{\gamma}{\nu} \simeq 1.95(0)$ which closely matches our estimation 1.94(4). Folk (2008) also predicted the critical exponents for tetracritical point with $\gamma = 1.36(6)$ and $\nu = 0.69(6)$. $\frac{\gamma}{\nu} \sim 1.96(3)$. Therefore, unfortunately we can not conclude if the exponent values are bicritial or tetracritical point at $T = 1.025$, but we do not have any evidence of the biconical structure so far.

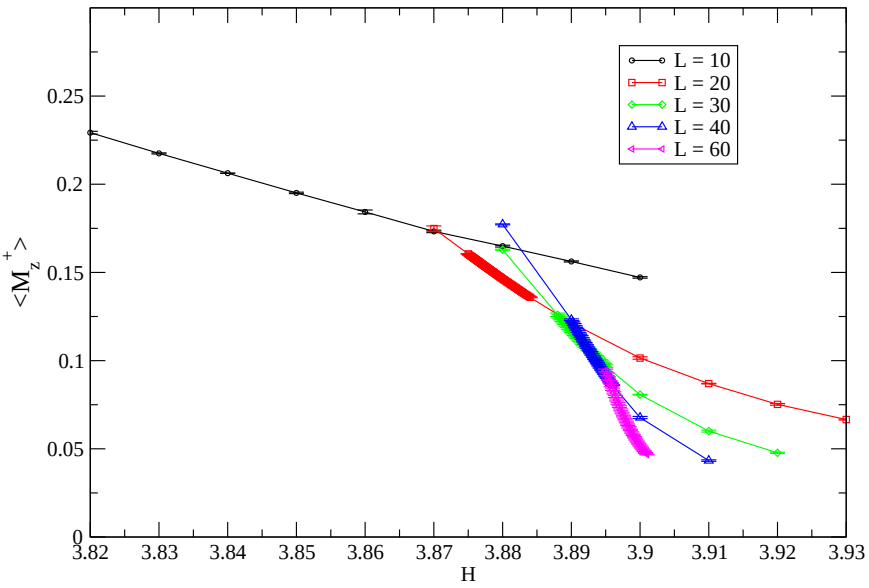

Figure 4.22: Order Parameter M_z^+ for $T = 1.025$, $\Delta = 0.8$

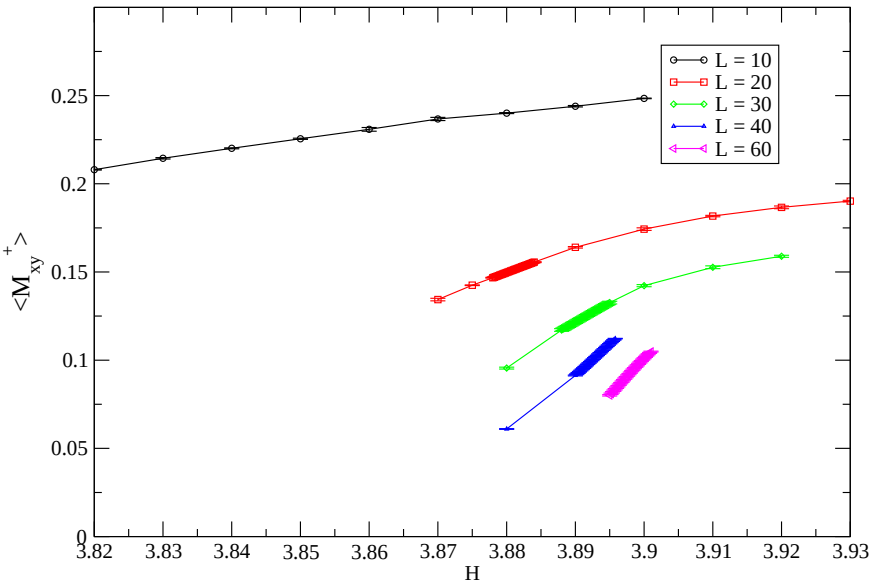

Figure 4.23: Order Parameter M_{xy}^+ for $T = 1.025$, $\Delta = 0.8$

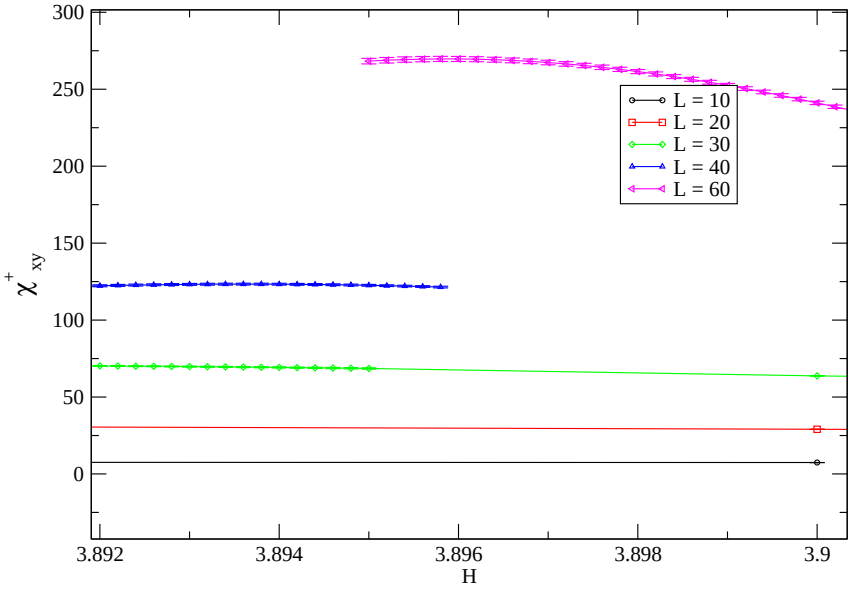

Figure 4.24: Susceptibility χ^+_{xy} for $T = 1.025$, $\Delta = 0.8$

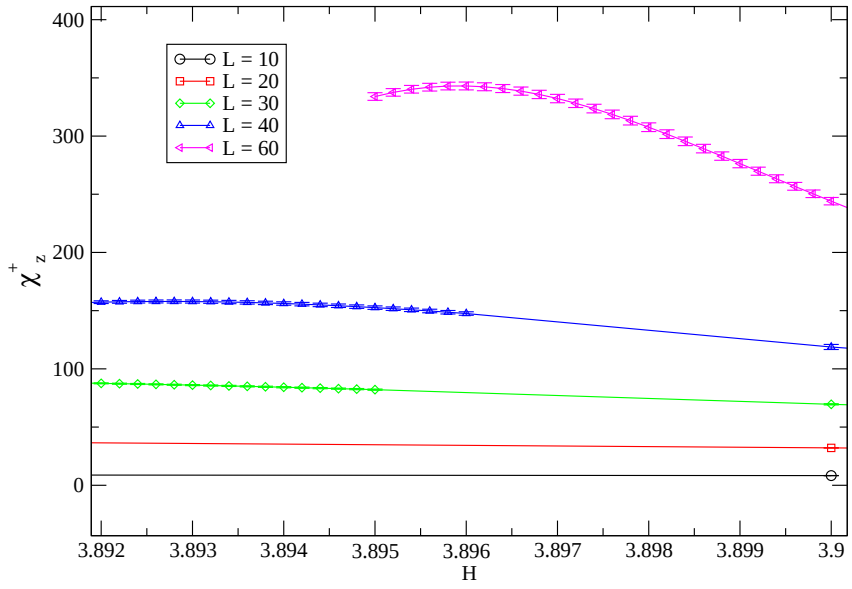

Figure 4.25: Susceptibility χ^+_z for $T = 1.025$, $\Delta = 0.8$

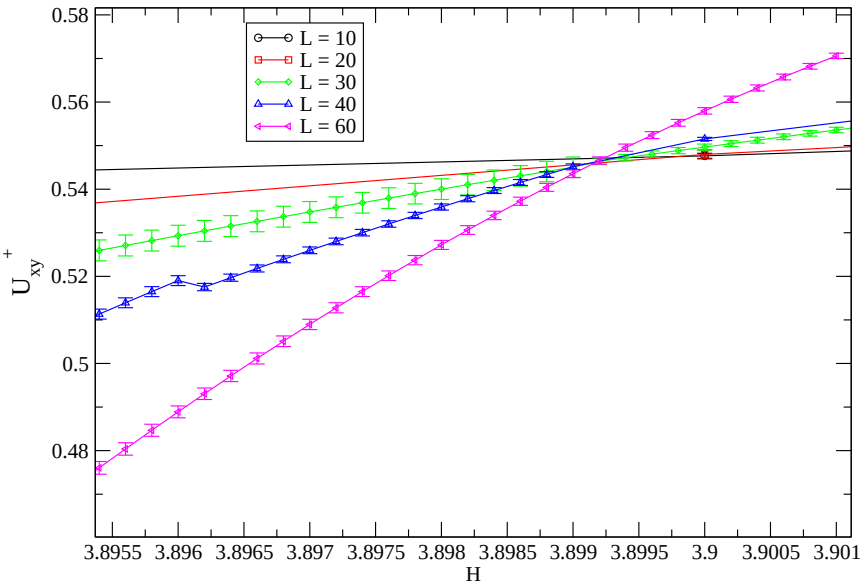

Figure 4.26: Cumulant U_{xy}^{+} for $T = 1.025$, $\Delta = 0.8$

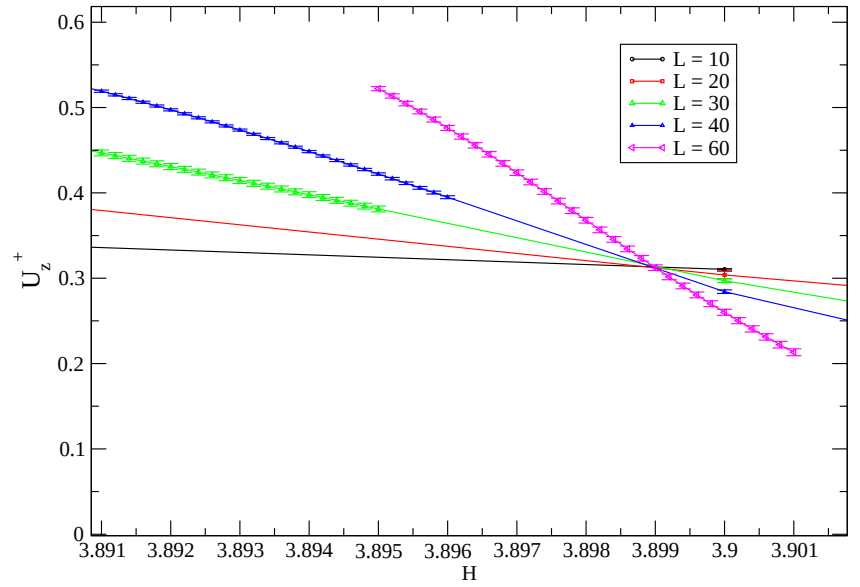

Figure 4.27: Cumulant U_{z}^{+} for $T = 1.025$, $\Delta = 0.8$

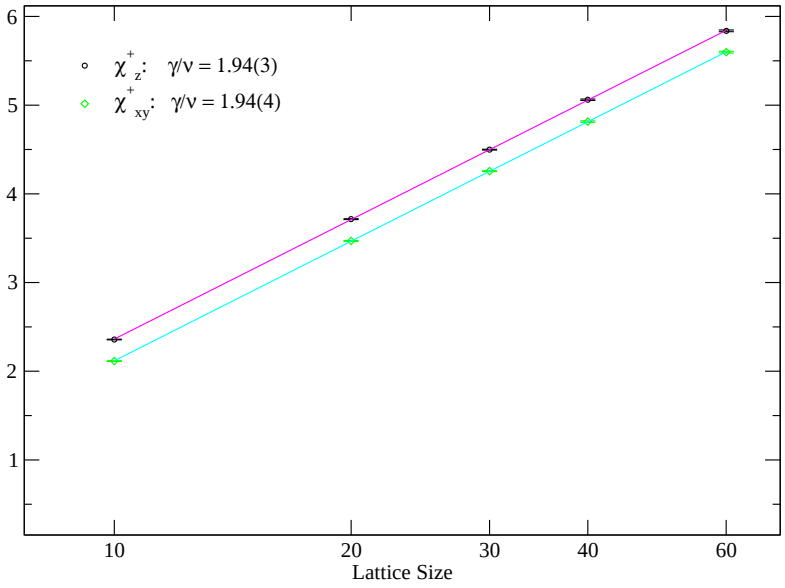

Figure 4.28: Finite Size Scaling for $T = 1.025$, the straight lines are fitted lines from data points

Chapter 5

Conclusion

We study the simple cubic lattice of a uniaxially antisotropic Heisenberg antiferromagnet in an external field H along with the z direction and examine the behavior which is close to the multicritical point. We search the biconical structures which is suspected to exist between the AF and SP phase and confirm the phase transition between Af and SF is the first order transition near the multicritical point.

We use Monte Carlo simulation method to generate data at different fields for $T = 0.95$, $T = 0.98$, $T = 1.01$. Red dots noted in Figure 5.1 show their locations in the phase diagram, respectively. We also adopt histogram reweighting to simulate thermodynamic behaviors near the phase transition. We focus on the quantities staggered susceptibilities χ_z^+, χ_{xy}^+, and Binder cumulants U_z^+ and U_{xy}^+. The finite size scaling demonstrates at different temperatures below $T = 1.025$, the phase transition belonexpect to detectgs to the first order transition. We also notice when the temperature we take comes close to the multicritical point, the crossover effect gets dominant which makes the first order transition behavior difficult to detect. In the end, we have no evidence to support the existence of two second order transitions and a biconical phases in between, but we do have evidence for a single first order transition ending in a multicritical point.

We also check the multicritical behavior at $T = 1.025$. It is hard to conclude if the critical exponents belong to 3D Heisenberg universality class or tetracritical universality class because both critical exponents are very close to each other. However, we do not find any existence of the biconical structure, which agrees with Selke (2011), and disagrees with the conclusion of Folk *et al*(2008). We conclude that the schematic picture of a first order

phase boundary ending in a bicritical point is likely to be correct, in disagreement with recent theoretical predictions. [18]

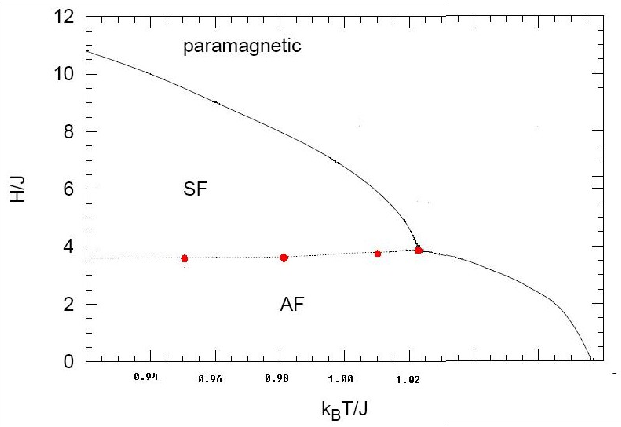

Figure 5.1: Data points we have analyzed at different temperatures in the phase diagram of the anisotropic antiferromagnet Heisenberg model with $\Delta = 0.8$. The lines separating AF and P, SF and P phases are second order transition lines, see Selke(2011)

Bibliography

[1] W.Selke, M.Holtschneider (2010), Physics Procedia, **6**, 84

[2] C.J.Gorter, T.Van Peski-Tinbergen (1956), PHysica, **22**, 273

[3] M.E.fisher, D.R. Nelson (1974), Phys. Rev. Lett. **32**, 1350

[4] G.Bannasch, W.Selke (2009), Euro. Phys. J. B**69**, 439-444

[5] J.M.Kosterlitz, D.R.Nelson (1976), Phys.Rev.B, **13**, 412

[6] W.Selke (2011), Phys. Rev.E, **83**, 042102

[7] M.Holtschneider, S.Wessel (2007), Phys. Rev. B, **75**, 224417

[8] M.E.J.Newmann, G.T.Barkema (1999), *Monte Carlo Methods in Statistical Physics*, Oxford University Press

[9] S.E.Koonin (1990), Computational Physics, Addison-Wesley Publishing company

[10] N.Metropolis *et al* (1953), J.Chem. Phys. **21**, 1087

[11] D.P.Landau, K. Binder (2000), A Guide to Monte Carlo Simulations in Statistical Physics, Cambridge University Press

[12] Alan M. Ferrenberg, Robert H. Swendsen(1988), Phys Rev.Lett, **61**,23

[13] M.E.Fisher, M.N.Barber (1972), Phys. Rev. Lett. **28**, 1516

[14] M.Fisher, A.N.Berker (1982), Phys. Rev. B. **60**, 487

[15] J.M.Yeomans (1992), *Statistical Mechanics of Phase Transitions*, Oxford University Press

[16] Jordan G.Bandkov (2000), Theory of Critical Phenomena in Finite Size Systems, World Scientific Publishing, Co. Ltd

[17] Kun Chen, A. Ferrenberg, D.P.Landau (1993), Phys. Rev. B, **48**, 5

[18] R.Folk,Yu.Holovatch *et al* (2008), Phys. Rev. E **78**, 041124